

Computer-Aided Acute Lymphoblastic Leukemia Diagnosis System Based on Image Analysis

Ahmed M. Abdeldaim, Ahmed T. Sahlol, Mohamed Elhoseny
and Aboul Ella Hassanien

Abstract Leukemia is a kind of cancer that basically begins in the bone marrow. It is caused by excessive production of leukocytes that replace normal blood cells. This chapter presents Computer-Aided Acute Lymphoblastic Leukemia (ALL) diagnosis system based on image analysis. It presented to identify the cells ALL by segmenting each cell in the microscopic images, and then classify each segmented cell to be normal or affected. A well-known dataset was used in this chapter (ALL-IDB2). The dataset contains 260 cell images: 130 normal and 130 affected by ALL. The proposed system starts by segmenting the white blood cells. This process includes sub-processes such as conversion from RGB to CMYK color model, histogram equalization, thresholding by Zack technique, and background removal operation. Then some features were extracted from each cell, each of them represents aspects of a cell. The extracted features include color, texture, and shape features. Then each feature set was exposed to three data normalization techniques z-score, min-max, and grey-scaling to narrow down the gap between the features values. Finally, different classifiers were used to validate the proposed system. The proposed diagnosing system achieved acceptable accuracies when tested by well-known classifiers; however, K-NN achieved the best classification accuracy.

A.M. Abdeldaim
Culture & Science City, 6th of October 15525, Egypt
e-mail: a7medabdeldaim@gmail.com

A.T. Sahlol (✉)
Damietta University, Damietta 34517, Egypt
e-mail: atsegypt@du.edu.eg

M. Elhoseny
Mansoura University, Mansoura, Egypt
e-mail: mohamed.elhoseny@unt.edu

A.E. Hassanien
Faculty of Computers and Information, Information Technology Department,
Cairo University, Giza, Egypt
e-mail: aboitcairo@gmail.com

A.M. Abdeldaim · A.T. Sahlol · M. Elhoseny · A.E. Hassanien
Scientific Research Group in Egypt (SRGE), Cairo, Egypt

Keywords Leukemia • Acute lymphoblastic leukemia (ALL) • Image analysis and segmentation • Data normalization

1 Introduction

Microscopic blood cell images enable doctors for diagnosing several diseases. Leukaemia can be considered as a type of blood cancer, it can be detected via the medical analysis of white blood cells or leucocytes. French–American–British (FAB) determined two types of leukaemia; Chronic, which are subclassified into Chronic Myelogenous Leukaemia (CML) and Chronic Lymphocytic Leukaemia (CLL). Acute, which is subclassified into: Acute Lymphoblastic Leukaemia (ALL) and Acute Myelogenous Leukaemia (AML) [1].

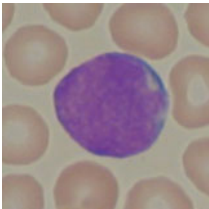
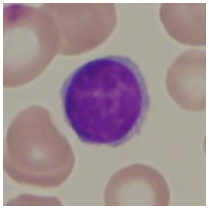
Acute lymphoblastic leukemia can be diagnosed by the morphological identification of lymphoblasts by microscopy, the immunophenotypic assessment of lineage commitment, and developmental stage by flow cytometry [2]. Blood samples can be observed and diagnosed for different diseases by doctors. Any human-based diagnosing suffers from nonstandard precision as it basically depends on doctor's skill; also it is unreliable in a statistical point of view. There are currently various systems that can count the number of blood cells based on measuring the physical and chemical properties of blood cells using a light detector that uses fluorescence or electrical impedance to identify cell types [3].

Although the quantification results are precise, it costs much money, also it does not detect the morphological abnormalities of the cells; therefore, a complementary blood analysis based on microscopic image is required. Image processing and their subsections like image segmentation can provide solutions for counting the number of cells in the blood, and accordingly, it can provide valuable information about cells morphology. Automated diagnosing systems are more accurate and not temperamental like human-based systems. Also, they are statistically reliable and can be generalized. So, the white blood cell (WBC) affected by acute lymphoblastic leukemia will be counted and classified.

There are three main components of blood image: red blood cells, platelets, and leucocytes. The red blood cells transport oxygen from the hurt to all organs and living tissues and in the same time, they carry away carbon dioxide. They are present at a percentage up to 50% of the total blood volume. RBCs' diameter is 6–8 μm . The WBCs play an important role in the body's immune system as they defend the body against infection and diseases. Therefore, analysis and classification of WBC are essential.

WBCs can be classified into two groups (by the presence of granules in the cytoplasm). The first group is Granulocytes, which includes basophil, eosinophil, and neutrophil. Basophil is responsible for allergic reaction and antigen, basophil's granules are of irregular distribution, they represent only 0–1% of all lymphocytes in human blood [4]. Eosinophil plays an important role in killing parasites, they present at 1–5% in human blood [5]. Neutrophil is most abundant in the blood stream.

Table 1 Normal and affected Lymphocyte cells

Type	Lymphocyte	
WBC	Normal cells	Affected cells
Samples from dataset [9]		

It has multiple-lobed nuclei, they present in human blood at a percentage ranging between 50 and 70% [6]. The second group is agranulocytes, it includes lymphocyte and monocyte. Lymphocyte is very common in human blood, with a percentage of 20–45% [7]. Monocytes are the largest WBCs; they represent 3–9% of circulating leucocytes [8].

Lymphocytes are regularly shaped and have a compact nucleus with regular and continuous edges. On the contrary, lymphocytes that are suffering from ALL are called lymphoblast. They are irregularly shaped and contain small cavities in the cytoplasm (termed vacuoles) and spherical particles within the nucleus (termed nucleoli), the more morphological changes increasing the more severity of the disease indicated [9]. Healthy and acute lymphoblastic leukemia lymphocytes are shown in Table 1.

Although, leukocytes can be easily identified (as they appear darker “purple” than the background), but due to wide variations in their shapes, dimensions, and edges, the analysis and the processing become very complicated. The generic term leucocyte refers to a set of cells that are quite different from each other. Thus, these cells can be distinguished according to their shape or size.

Image analysis techniques were adopted in several fields; medical [10–12] and others [13, 14]. Mohapatrain [15] used an ensemble classifier system for the early diagnosis of acute lymphoblastic leukemia in blood microscopic images. The identification and segmentation of WBCs were done followed by extracting different types of features. Features covered most aspects of WBC such as shape, contour, fractal, texture, color, and Fourier descriptors. Finally, an ensemble of classifiers is trained to recognize acute lymphoblastic leukemia. The results of this method were good, however, the reproducibility of the experiment and comparisons with other methods are not possible as the dataset was not available for public. In [16], it was proposed a technique to segment the acute leukemia cell images by transforming the RGB color space to C-Y color space in the C-Y color space, the luminance component is used to segment (ALL). The proposed algorithm runs on 100 microscopic ALL images and the experimental result shows that it achieved a good segmentation of ALL from its complicated background, as the segmentation accuracy reached 98.38%.

While in [17], two sets of blood WBC images were used in this study's experiments. The first contains 555 images with 601 white blood cells. They were collected from Rangsit University. The second contains 477 cropped WBC images which were downloaded from CellaVision.com. The proposed system comprises a preprocessing step, nucleus segmentation, cell segmentation, feature extraction, feature selection, and classification. Naïve Bayes classifiers were applied for performance comparison. It was found that the proposed method is consistent and coherent in both datasets, with dice similarity of 98.9 and 91.6% for average segmented nucleus and cell regions, respectively. Furthermore, the overall correction rate in the classification phase is about 98 and 94% for linear and naïve Bayes models, respectively.

In [18], an automated blast counting method to detect acute leukemia in blood microscopic images was proposed to identify the WBCs through a thresholding operation performed on the HSV color space S component. Morphological erosion for image segmentation was done. The results of this study were promising; however, no features or classifiers were presented. Also, there is no method to determine the optimum threshold for segmentation. Also in [3], the whole leucocyte was isolated and then the nucleus and cytoplasm were separated, then different features, such as shape, color, and texture are extracted. The feature set was used to train different classification. 245 of 267 total leucocytes were properly identified (92% segmentation accuracy). Different classification models were tested; however, the support vector machine with a Gaussian radial basis kernel has the highest performance for the identification of acute lymphoblastic leukemia by achieving a 93% of accuracy and a 98% of sensitivity.

In this chapter, it is focused only on the acute lymphoblastic leukemia (ALL), which is well known as it affects basically children and older people. Children under 5 years and older people over 50 years are at higher risk of acute lymphoblastic leukemia, also, it can be fatal if it is not treated earlier as it is rapidly spread into some vital organs and the bloodstream too [19]. Therefore, earlier diagnosis greatly aids in providing the appropriate treatment for ALL and is developing a fully automated computer-aided diagnosis system for detection, segmentation, feature extraction, and classification of WBCs affected by acute lymphoblastic leukemia. The system inputs are microscopic images (some affected by ALL while others not), and the decision is taken by the model is the identifying whether each image is suffering from acute lymphoblastic leukemia or not.

The remainder of this chapter is presented as follows. Section 1 gives an overview of the related works; Sect. 2 describes in details the proposed system. The results and discussions are presented in Sect. 3. Finally, the conclusions and future chapter are discussed in Sect. 4. The proposed computer-aided acute lymphoblastic leukemia diagnosis system.

2 The Proposed System

The proposed computer-aided acute lymphoblastic leukemia diagnosis system aims to optimally select the most powerful features that can be used in the lymphoblastic leukemia diagnosis system. The proposed lymphoblastic leukemia diagnosis system consists of three basic phases: Image segmentation, feature extraction, and classification. The overall architecture of the proposed system and its phases are summarized in Fig. 1.

2.1 Cell Segmentation Phase

Unlike many methods in the literature, the proposed system detects the nuclei and the entire membrane at the same time.

Each image in the dataset contains only one cell. The images are in RGB color space which is difficult to be segmented. So, the images were converted to CMYK color space (Eqs. 1–4). In fact, leukocytes are more contrasted in the Y component of CMYK color model because the yellow color is presented in all elements of the image; then Y was used as the whole cell and M as the nucleus.

$$K = \min(255 - r, \min(255 - G, 255 - B)) \quad (1)$$

$$C = \frac{255 - R - K}{255 - K} \quad (2)$$

$$M = \frac{255 - G - K}{255 - K} \quad (3)$$

$$Y = \frac{255 - B - K}{255 - K} \quad (4)$$

For Y component, segmentation is a bit easier because the whole cell exists in pure black color; so the non-black elements were ignored in the image. However, for M component, it was a bit challenging because of the variation of magenta color levels in the image. Therefore, as in [3], the segmentation was performed by Zack algorithm [20] which was used to determine the thresholding value. Before it is applied, a histogram for the grayscale cell image has to be produced then the intensity values of it are exposed to the Zack's. The thresholding value estimation by Zak's can be calculated by constructing a line between the maximum (a) and the minimum (b) of the histogram grey level axis, where the minimum (b) is larger than 0. The distance (L) which is the length between the line and the histogram is computed for all values between (b) and (a). The thresholding value is the value of the grey intensity axis when the distance (L) reaches its maximum value. This algorithm is particularly effective when the object pixels produce a weak peak in the histogram. Figure 2 shows how threshold value can be calculated by Zack algorithm.

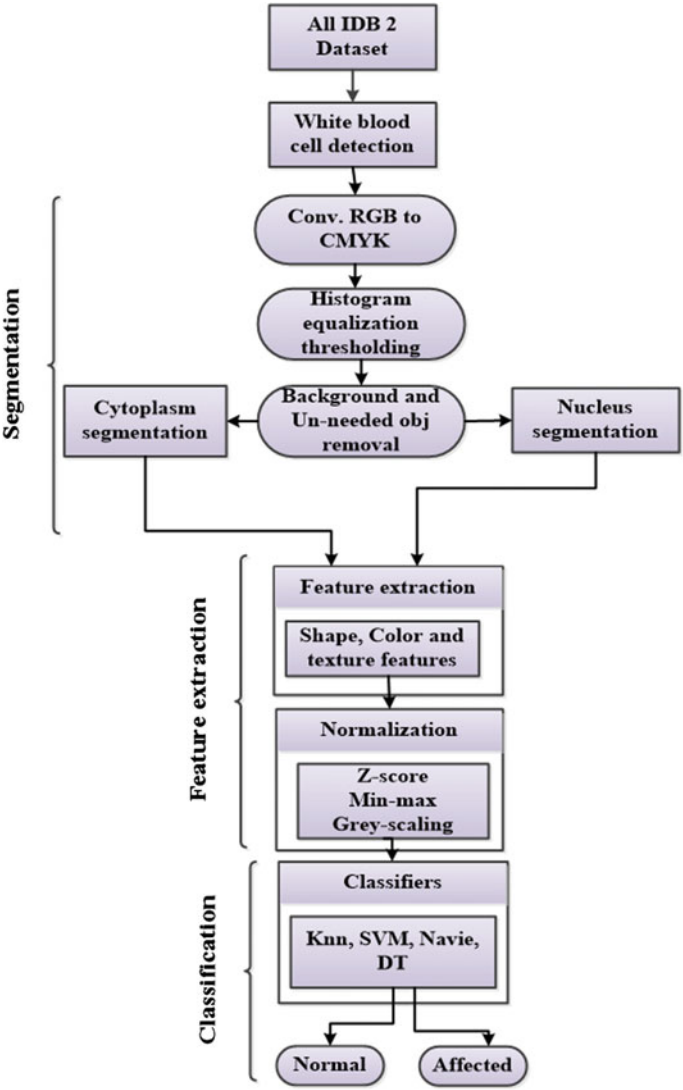


Fig. 1 The proposed lymphoblastic leukemia diagnosis System

Cleaning the image edge is a simple task. In this chapter, in order to remove the nonlymphocyte cells, the roundness equation (Eq. 5) was used, as the lymphocyte cell has a unique circular shape, so it measures how closely the morphology of a shape to be a circle is. Roundness is dominated by the shape's gross features rather

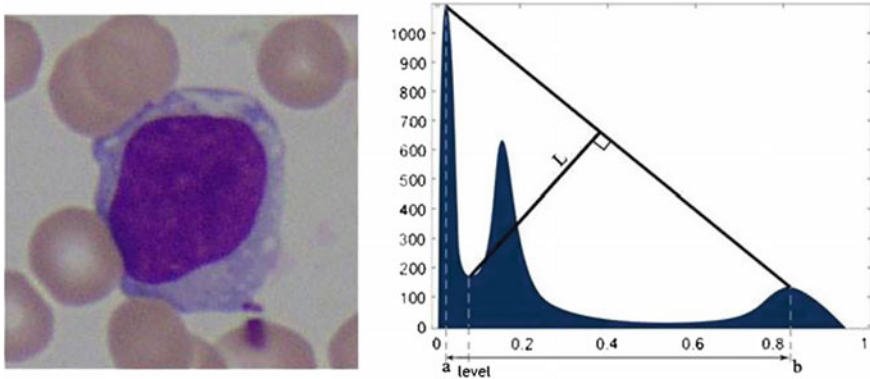


Fig. 2 First Image from the data set. Second threshold calculated by Zack's

than the definition of its edges and corners, or the surface roughness of a manufactured object:

$$\text{Roundness} = \frac{4 \times \pi \times \text{Area}}{\text{Convex Perimeter}} \quad (5)$$

If roundness is equal to 1 then the shape is circular, the closer the roundness to 1 the closer the shape has a circular shape. Roundness is relatively insensitive to irregular boundaries. After several trials on the images, it was assumed that the best minimum roundness value for a Lymphocyte cell is 0.52. Beside roundness, the solidity of the object, solidity (Eq. 6) was calculated. It can be defined as the ratio of the area of an object to the area of a convex hull of an object.

$$\text{Solidity} = \frac{\text{Area}}{\text{Convex Area}} \quad (6)$$

A solidity value of 1 signifies a solid object, and a value less than 1 represents that an object has an irregular boundary (or containing holes). After several trials, it was considered the minimum value of solidity for a lymphocyte cell is to be 0.98.

So, if the roundness and the solidity of an object are more than the assumed values then this object classified is as a lymphocyte cell and it proceeds to the final step, otherwise, it does nothing. Filling hole method [20] was used to recover images from distortion of important pixels resulted after the previous preprocessing operations.

2.2 Feature Extraction Phase

Feature extraction in image processing is a technique of transforming the input data into the set of features. In order to construct an effective feature set, several published articles were studied, it was noted that certain features were widely used as they gave good classification results. Three types of features were extracted from the segmented cells including shape features, color features, and texture features. Table 2 summarizes the all extracted features and their numbers.

2.2.1 Shape Features

Starting from binary images of the nucleus and the nucleus with cytoplasm, the extracted shape features include: Area, Perimeter, Major Axis Length, Minor Axis Length, Convex Area, Convex Perimeter, Orientation, Roundness, Solidity, Elongation, Eccentricity, Rectangularity, Compactness, Convexity, and the Area Ratio. All these features were calculated for two types of images (nucleus and nucleus with cytoplasm). In this chapter, 30 shape features were extracted.

2.2.2 Color Features

The color features are the most discriminatory features of blood cells. The mean, standard deviation, skewness, kurtosis, and entropy were calculated from the three channels (red, green, blue) of each image. The extracted color features included only 15 features.

2.2.3 Texture Features

The texture features were extracted from each cell image in the grey level format. The following descriptors were evaluated: Autocorrelation, Contrast, Correlation, Cluster Prominence, Cluster Shade, Dissimilarity, Energy, Homogeneity 1, Homogeneity 2, Maximum Probability, Sum of Squares Variance, Sum Average, Sum Variance, Sum Entropy, Difference Variance, Difference Entropy, Information Measure of Correlation 1, Information Measure of Correlation 2, Inverse Difference is Homom, Inverse Difference Normalized, and Inverse Difference Moment Normalized. These features

Table 2 Types of the extracted features

Feature type	Numbers
Color features	15
Shape features	30
Texture feature	84

were calculated for the 0, 45, 90, and 135 angles. The extracted texture feature set contains 84 features.

Unfortunately, the shape features cannot only be trusted because they are sensitive to segmentation errors. Thus, these features were combined together with regional features, which are less susceptible to errors. We have one more feature set that was hybridized by color and texture features. The combination of shape, color, and texture features produces a feature set of 129 features.

2.3 Feature Normalization

To narrow down the gap between the highest and the lowest value of extracted features and to improve the classification results. Three different normalization techniques were applied; they include grey-scaling, min-max and Z-score techniques.

2.3.1 Grey-Scaling

It is an image normalization technique used to convert a matrix to a greyscale image. This can be performed by scaling the entire image to the range of brightness values from 0 to 1. It works by normalizing each individual columns or rows to a range of brightness values from 0 to 1.

2.3.2 Min-Max

Data are scaled to a fixed range usually 0–1. The cost of having this bounded range in contrast to standardization is that it will be ended up with smaller standard deviations, which can suppress the effect of outliers. Min-max scaling (Eq. 7) is typically done via the following equation:

$$X_i = \frac{X_i - X_{\min}}{X_{\max}}, \quad (7)$$

where X_i is the original feature vector, X_{\min} is the minimum value of that feature vector, and X_{\max} is the maximum value of it.

2.3.3 Z-Score

In this normalization method, the mean and the standard deviation of each feature are calculated (Eq. 8). Next, the mean was subtracted from each feature. Finally, the product values were divided by the standard deviation.

$$Z_i = \frac{X_i - \bar{X}}{\sigma}, \quad (8)$$

where X_i is the original feature vector, \bar{X} is the mean of that feature vector, and σ is its standard deviation.

2.4 Classification Phase

The proposed system can be considered a binary classification problem because there are only two classes (normal or affected cell) as outputs and number of variables (features) as inputs. In this chapter, as there are different number of features (starting from 5 to 127), several classifiers were used. The extracted feature sets were tested by k-Nearest Neighbor (k-NN) [21] using the Euclidean distance measure with different values of k, Naive Bayes (NB) [22, 23], by a Gaussian (G) and kernel data distribution (K), support vector machines [24] with different kernels and Decision Trees [25]. The chosen classifiers proved to achieve acceptable results with other pattern recognition problems [26, 27]. The performance of the models was evaluated using a k-fold, cross validation. Considering $k = 10$, the whole dataset is randomly divided into tenfolds.

3 Experimental Results and Discussions

The proposed system was implemented by “MATLAB 2016b” on “Windows 7 (64 bit)”. The dataset was provided by Department of Information Technology – Università degli Studi di Milano [9]. The dataset was captured with an optical laboratory microscope coupled with a Canon PowerShot G5 camera. All images are in JPG format with 24-bit color depth. The images were taken with a different magnification of microscope ranging from 300 to 500. The ALL-IDB database has two distinct versions (ALL-IDB1 and ALL-IDB2). The proposed system worked on the ALL-IDB2 version which has been designed for testing the performances of classification systems. The ALL-IDB2 is a collection of cropped area of interest of normal and blast cells that belongs to the ALL-IDB1 dataset. It contains 260 images, half of them lymphoblast's. ALL-IDB2 images have similar grey level properties to the images of the ALL-IDB1, except the image dimensions.

The accuracy (Eq. 9) was used to test the classification performance of the proposed system:

$$\text{Accuracy} = \frac{TP + TN}{TP + TN + FP + FN}, \quad (9)$$

where

- TP (True positives) is the number of elements that are correctly classified as positive by the test.
- TN (True negatives) is the number of elements that are correctly classified as negative by the test.
- FP (False positive) is also known as type I error, it is the number of elements that are classified as positive by the test, but they are not.
- FN (True positive) is also known as type II error, it is the number of elements that are classified as negative by the test, but they are not.

In order to investigate the performance of the segmentation, the output of the segmentation process was compared to that was provided by the data set truth table. Figures 3, 4 and 5 show the segmentation results of some images from the data set.

The segmentation accuracy was tested using (Eq. 9) and the achieved accuracy reached 99.2%, represents 189 true positives, 69 true negatives, 2 false positives, and there were no false negative cell images out of 260 cell images. As mentioned, the proposed system produced several feature sets (six feature sets). Each was exposed to three data normalization techniques, so 18 feature sets were produced. Tables 3, 4, 5, 6, 7, and 8) represent the classification accuracy of each of the extracted feature sets when tested by k-nearest neighbor, Naive Bayes by a Gaussian (G), and kernel data distribution (K), support vector machines and decision trees classifiers.

In order to investigate the performance of the used classifiers, the best classification accuracy achieved by each of them was presented, as seen in Fig. 7.

From Fig. 7, it is obvious that the classification accuracy did not go lower than 86%; however, the best classifier was K-NN. This matches with our previous work [28], that K-NN has several parameters like the distance function as well as the number of neighbors that can adapt the learning mechanism toward improving the classification performance. As three normalization techniques were adopted in this

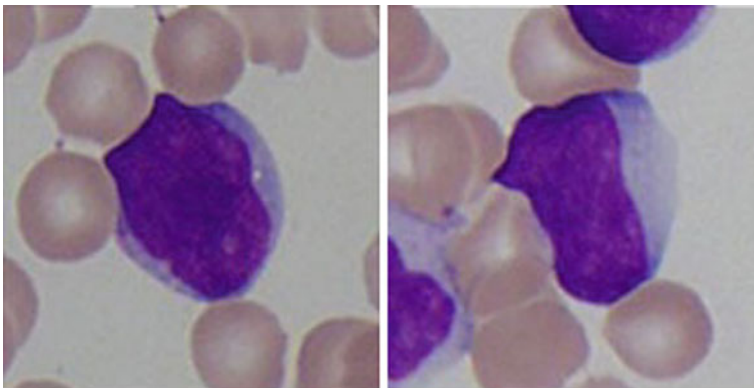


Fig. 3 Samples of the data sets

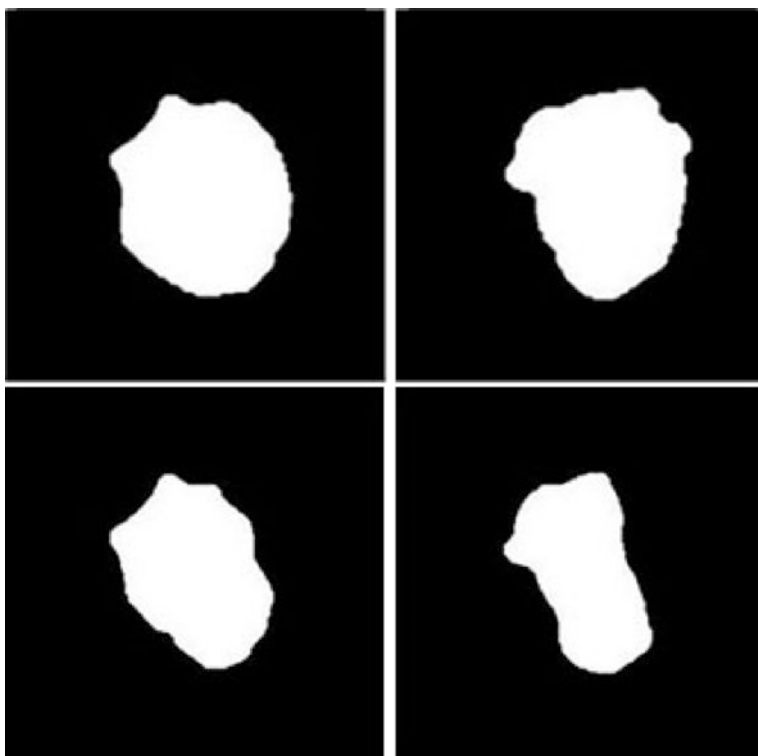


Fig. 4 Leucocyte segmentation. *Up* whole leucocyte images. *Down* nucleus images

chapter, so a comparison between the best and the worst classification accuracy for each of them is shown in Fig. 8.

Figure 8 shows the three used normalization techniques and the best and the worst classification accuracy. It is seen that they have almost the same performance for the best experiment; however, the grey-scaling has the best accuracy of the worst experiments.

The performed experiments included also the relationship between the number of features and the classification accuracy. Figure 9 shows the relationship between the number of features and the achieved accuracy.

From Fig. 9, it is noted that the accuracy gets better the when number of features increased for all the used classifiers. Also, the worst accuracy did not go lower than 80% except for the Naive Bayes. It is also noticed that the gap between the lowest and the highest number of features in terms of accuracy is not high as it does not exceed 5%.

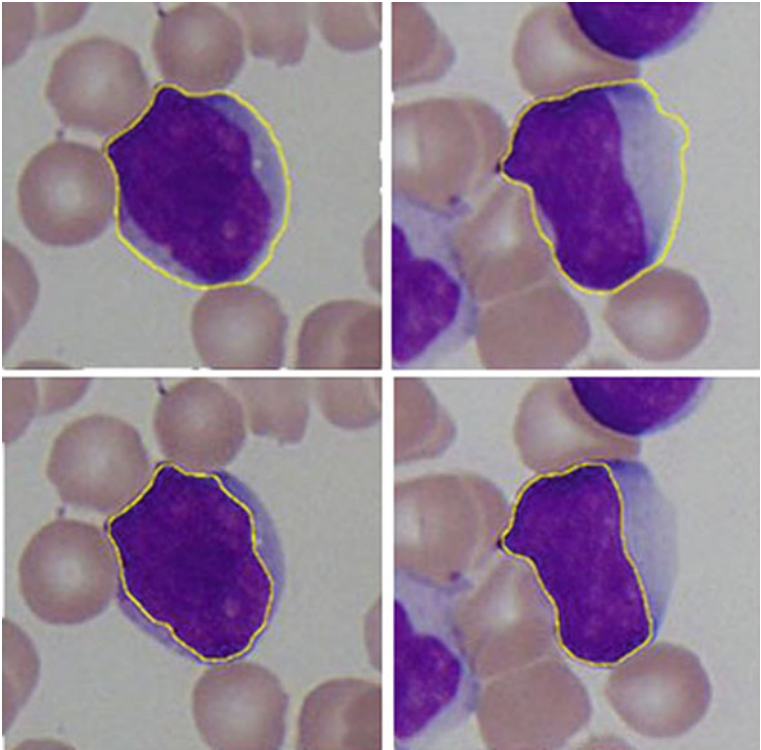


Fig. 5 Leucocyte identification (border highlighted). *Up* whole leucocyte cell images. *Down* nucleus cell images

Table 3 Classification performance of some texture features with the three normalization techniques

Classifier	Grey-scaling	Z-Score	Min-max
Knn	95.78	88.82	89.25
SVM-RBF	90.87	89.27	83.64
SVM-L	89.07	89.87	68.35
SVM-P	92.18	90.56	88.46
NB-G	83.5	82.12	78.3
NB-K	86.14	86.78	81.94
TREE	88.48	88.59	86.13

Table 4 Classification performance of all texture features with the three normalization techniques

Classifier	Grey-scaling	Z-Score	Min-max
Knn	90.94	95.99	92.57
SVM-RBF	91.49	69.77	93.41
SVM-L	90.14	92.55	89.58
SVM-P	88.96	87.83	92.51
NB-G	79.66	84.09	84.4
NB-K	82.7	86.81	86.44
TREE	79.66	89.28	85.47

Table 5 Classification performance of some color features with the three normalization techniques

Classifier	Grey-scaling	Z-Score	Min-max
Knn	88.95	88.66	87.96
SVM-RBF	82.38	88.12	77.97
SVM-L	77.7	86.98	69.75
SVM-P	85.4	88.77	86.08
NB-G	80.58	83.14	72.89
NB-K	82.24	82.29	77
TREE	88.02	85.43	85.09

Table 6 Classification performance of all color features with the three normalization techniques

Classifier	Grey-scaling	Z-Score	Min-max
Knn	86.93	89.63	87.57
SVM-RBF	87.53	89.83	88.45
SVM-L	72.43	81.52	73.48
SVM-P	91.62	90.35	92.52
NB-G	72.16	77.61	76.89
NB-K	79.52	80.23	79.38
TREE	84.51	85.715	89.41

Table 7 Classification performance of colors and texture features with the three normalization techniques

Classifier	Grey-scaling	Z-Score	Min-max
Knn	96.42	90.69	93.63
SVM-RBF	94.41	65.3	93.57
SVM-L	92.51	93.73	95.34
SVM-P	94.06	88.59	94.87
NB-G	87.85	82.83	90.34
NB-K	85.73	83.3	89.45
TREE	84.59	82.15	90.93

Table 8 Classification performance of colors, shape and texture features with the three normalization techniques

Classifier	Grey-scaling	Z-Score	Min-max
Knn	96.01	84.69	81.38
SVM-RBF	92.80	65.98	82.68
SVM-L	93.43	91.54	89.05
SVM-P	93.89	89.01	91.15
NB-G	89.97	82.81	83.89
NB-K	86.02	81.99	82.62
TREE	86.81	82.29	81.55

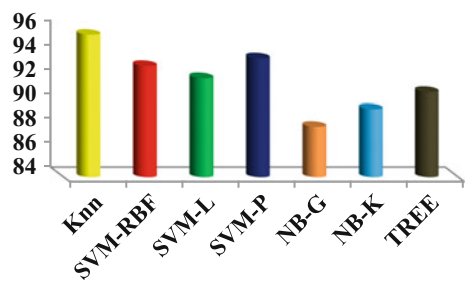


Fig. 7 Different accuracies based on different classifiers

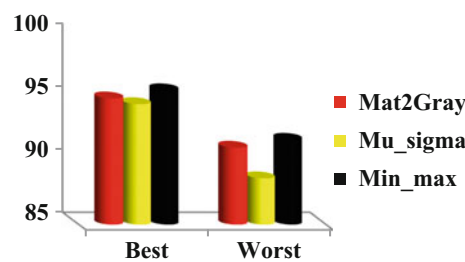


Fig. 8 Different accuracies based on different normalization methods

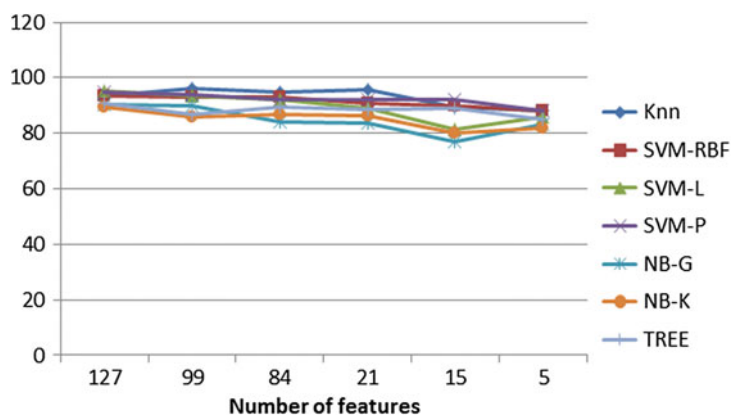


Fig. 9 Different accuracies based on different number of features

4 Conclusions and Future Works

This chapter focused on lymphocyte cells which are affected by lymphoblastic cancer. The main objective of this chapter is to identify the lymphocyte by segmenting the microscopic images then diagnose (classify) each segmented cell to be normal or affected. The ALL-IDB2 published dataset was used in this chapter to test the efficiency of the proposed diagnosis system. The dataset contains 260 cell images; 50% are normal, and the rest 50% are affected by ALL. The proposed system starts with segmentation which included the conversion from RGB to CMYK color model then contrast stretching by histogram equalization then thresholding and noise removal including background removal operation. Second, some features were extracted from each cell. They can be classified as color, texture, and shape features. Third, three data normalization techniques (z-score, min-max and grey-scaling) were applied to each extracted features to improve the classification performance. Finally, different classifiers were used (K-Nearest Neighbor, Naive Bayes, Support vector machines and Decision Trees) to test the efficiency of the proposed system. The performance of the proposed system was acceptable in terms of the segmentation performance as well as the accuracy of all classifiers, especially K-NN which achieved the best classification accuracy. The future work might include the extension of this chapter to cover the other kind of white blood cancers.

References

1. Bennett, J.M., Catovsky, D., Daniel, M.T., Flandrin, G., Galton, D.A., Gralnick, H.R., et al.: Proposals for the classification of the acute leukemias. French–American–British (FAB) co-operative group. *Br. J. Hematol.* (1976)
2. Inaba, H., Greaves, M., Mullighan, C.G.: Acute lymphoblastic leukaemia. *Lancet* **381**, 1943–1955 (2013)
3. Putzu, L., Caocci, G., Di Ruberto, C.: Leucocyte classification for leukaemia detection using image processing techniques. *Artif. Intell. Med.* **62**, 179–191 (2014)
4. Qiu, H.N., Wong, C.K., Chu, I.M., Hu, S., Lam, C.W.: Muramyl dipeptide mediated activation of human bronchial epithelial cells interacting with basophils: a novel mechanism of airway inflammation. *Clin. Exp. Immunol.* **172**, 81–94 (2013)
5. Meeusen, E.N., Balic, A.: Do eosinophils have a role in the killing of helminth parasites?. *Parasitol. Today* **16**, 95–101 (2000)
6. Kolaczowska, E., Kubes, P.: Neutrophil recruitment and function in health and inflammation. *Nat. Rev. Immunol.* **13**, 159–175 (2013)
7. Thompson, S.C., Bowen, K.M., Burton, R.C.: Sequential monitoring of peripheral blood lymphocyte subsets in rats. *Cytometry* **7**, 184–193 (1986)
8. Brown, A.L., Zhu, X., Rong, S., Shewale, S., Seo, J., et al.: Omega-3 fatty acids ameliorate atherosclerosis by favorably altering monocyte subsets and limiting monocyte recruitment to aortic lesions. *Arterioscler. Thromb. Vasc. Biol.* **32**, 2122–2130 (2012)
9. DonidaLabati, R., Piuri, V., Scotti, F.: ALL-IDB: The acute lymphoblastic leukemia image data base for image processing. In: *The 18th IEEE International Conference on Image Processing (ICIP)*, pp. 2045–2048 (2011)

10. Mostafa, A., Fouad, A., Elfattah, M.A., Hassanien, A.E., Hefny, H., Zhu, S.Y., Schaefer, G.: CT liver segmentation using artificial bee colony optimisation. *Procedia Comput. Sci.* **60**, 1622–1630 (2015)
11. Zidan, A., Ghali, N.I., Hassanien, A.E., Hefny, H., Hemanth, J.: Level set-based CT liver computer aided diagnosis system. *J. Intell. Robot. Syst.* **7**, Number S13 (2012)
12. Anter, A.M., Hassenian, A.E., ElSoud, M.A., Tolba, M.F.: Neutrosophic sets and fuzzy C-means clustering for improving CT liver image segmentation. In: *The 5th International Conference on Innovations in Bio-Inspired Computing and Applications*, Ostrava, Czech Republic, 22–24 June 2014
13. Sahlol, A.T., Suen, C.Y., Zawbaa, H.M., Hassanien, A.E., Elfattah, M.A.: Bio-inspired BAT optimization algorithm for handwritten arabic characters recognition. In: *2016 IEEE Congress on Evolutionary Computation (WCCI-2016)*, Vancouver, Canada, pp. 1749–1756, 22–24 July 2016
14. Elhoseny, M., Farouk, A., Batle, J., Abouhawwash, M., Hassanien, A.E.: Secure image processing and transmission schema in cluster-based wireless sensor network. In: *Handbook of Research on Machine Learning Innovations and Trends* (2017)
15. Mohapatra, S., Patra, D., Satpathy, S.: An ensemble classifier system for early diagnosis of acute lymphoblastic leukemia in blood microscopic images. *J. Neural Comput. Appl.* **24**(7–8), 1887–1904 (2014)
16. Mohammed, R., Nomir, O., Khalifa, I.: Segmentation of acute lymphoblastic leukemia using C-Y color space. *Int. J. Adv. Comput. Sci. Appl. (IJACSA)* **5**(11), 99–101 (2014)
17. Prinyakupt, J., Pluempitiwiriyaew, C.: Segmentation of white blood cells and comparison of cell morphology by linear and naïve Bayes classifiers. *Biomed. Eng. OnLine* **14**(1), 63 (2015)
18. Halim, N.H.A., Mashor, M.Y., Hassan, R.: Automatic blasts counting for acute leukemia based on blood samples. *Int. J. Res. Rev. Comput. Sci.* **2**(4), 971–976 (2011)
19. Biondi, A., Cimino, G., Pieters, R., Pui, C.H.: Biological and therapeutic aspects of infant leukemia. *Blood* **96**, 24–33 (2000)
20. Zack, G., Rogers, W., Latt, S.: Automatic measurement of sister chromatid exchange frequency. *J. Histochem. Cytochem.* **25**(7), 741–753 (1977)
21. Cover, T.M., Hart, P.E.: Nearest neighbor pattern classification. *IEEE Trans. Inf. Theory* **13**, 21–27 (1967)
22. Duda, R.O., Hart, P.E.: *Pattern Classification and Scene Analysis*. Wiley, New York (1973)
23. Langley, P., Iba, W., Thompson, K.: An analysis of Bayesian classifiers. In: Rosenbloom, Paul, Szolovits, Peter (eds.) *Proceedings of the Tenth National Conference on Artificial Intelligence*, pp. 223–228. The AAAI Press, Menlo Park, CA (1992)
24. Vapnik, V.: *Statistical Learning Theory*. Wiley (1998)
25. Quinlan, J.R.: Induction of decision trees. *Mach. Learn.* (1986)
26. Sahlol, A.T., Suen, C.Y., Zawbaa, H.M., Hassanien, A.A., AbdElfattah, M.: Bio-inspired BAT optimization technique for handwritten Arabic characters recognition. In: *IEEE Congress on Evolutionary Computation (WCCI-2016)*, Vancouver, Canada, pp. 1749–1756 (2016)
27. Sahlol, A.T., AbdElfattah, M., Suen, C.Y., Hassanien, A.A.: Particle swarm optimization with random forests for handwritten Arabic recognition system. In: *Proceedings of the International Conference on Advanced Intelligent Systems and Informatics (AISIS 2016)*, Cairo, Egypt, pp. 437–446 (2016)
28. Sahlol, A.T., Suen, C.Y., Elbasyoni, M.R., Sallam, A.A.: Investigating of preprocessing techniques and novel features in recognition of handwritten Arabic characters. In: *Artificial Neural Networks in Pattern Recognition*, pp. 264–276. Springer International Publishing (2014)
29. Soille, P.: *Morphological Image Analysis: Principles and Applications*, pp. 170–171. Springer (1999)